Conclusion

For a rectangular, σ-aromatic cyclobutane dication, like the pagodane or the norbornadiene dication, to be stable, some prerequisites are essential:

(1) A rigid molecular framework is needed to prevent in-plane distortion toward the rhomboid form or out of plane motion toward D_{2d} symmetry (imaginary vibrational frequency modes of the parent compound **11**, Figure 4).

(2) The two formal ethylene radical cation units have to be held at distances between ~1.9 and 2.3 Å to keep the diradicaloid character low enough to prevent side reactions.

Another conclusion can be drawn from the numerous experiments aimed at oxidizing cyclobutane containing compounds: the cyclobutane system has to be octasubstituted, perhaps due to both kinetic and thermodynamic stabilization.[34]

The pagodane dication and the norbornadienyl dication can be viewed as frozen aromatic transition states of the reaction of two ethylene radical cations in the sense of the Dewar/Evans principle.[16] A cycloaddition of two neutral ethylene molecules in D_{2h} symmetry is forbidden because the transition state would be antiaromatic (triplet diradical), while the product cyclobutane again is closed shell. Removing two electrons from the system reverses the picture. The educts are two ethylene radical cations, the transition state is aromatic (almost pure closed shell), and the product, the square cyclobutane dication, again is diradical. The formal transition state now is a minimum on the reaction path within D_{2h} symmetry because of its aromatic stabilization. This stabilization, however, has to be paid for by a strong Coulomb repulsion of the two positive charges. If the system is not constrained within a D_{2h} symmetry by a rigid molecular framework, the charges will be separated by distortion toward a rhomboid or tetrahedral geometry and bishomoaromaticity will be canceled. Hence, it should be possible to synthesize molecules corresponding to some other points on the reaction coordinate and thus test the limits of homoaromaticity.

The rectangular cyclobutane dication is also interesting from another point of view. It is the third in a set of topologically different two-electron four-center hydrocarbon aromatic compounds, which have been verified experimentally.

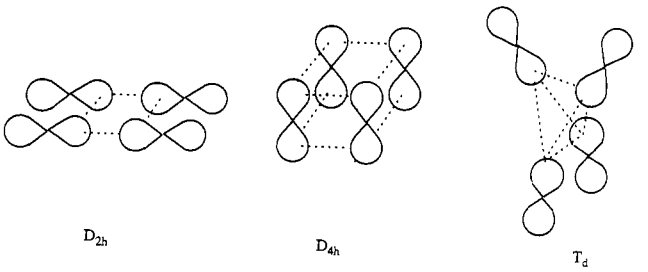

None of these ideal arrangements is an energy minimum without extra stabilization by substitution. The square D_{4h} cyclobutadiene dication is a transition state for the ring inversion of the puckered structure.[21a,35] The tetrahedral dication needs six CH_2 bridges on all edges of the tetrahedron (realized in the adamantane framework)[21b] to be a relative minimum on the energy hypersurface. Their instability notwithstanding, such dications can serve as models illustrating the concepts of aromaticity and isolobal structures.

Acknowledgment. We thank the Fonds der Chemischen Industrie for support through a Liebig Stipendium to R.H. GAUSSIAN82 calculations were carried out on a CONVEX C1; we thank the CONVEX Computer Corp. for support, the Leibniz Rechenzentrum in Munich for providing supercomputing time on a CRAY X-MP/24 and a Cray Y-MP4/432, and Dr. A. J. Kos for early calculations on $C_4H_8^{2+}$.

Registry No. 4, 99828-64-5; **15**, 132646-10-7; ethylene radical cation, 34470-02-5; 1,4-butanediylium, 111160-98-6; norbornadiene dication, 132832-60-1.

Supplementary Material Available: Full calculational details of ab initio calculations of **4**, **13**, **14**, and **15** (20 pages). Ordering information is given on any current masthead page.

(34) Norbornadiene or quadricyclane cannot be oxidized to form the corresponding dication. Reaction with SbF_5 in SO_2ClF even at very low temperatures occurs violently to form black polymers. Herges, R.; Prakash, G. K. Unpublished results. For other unsuccessful attempts to oxidize cubane, homocubane, bishomocubane, and related, not fully substituted cyclobutane systems, see: ref 2, p 7767.

(35) (a) Olah, G. A.; Bollinger, J. M.; White, A. M. J. *J. Am. Chem. Soc.* **1969**, *91*, 3667. (b) Olah, G. A.; Mateescu, G. P. *Ibid.* **1970**, *92*, 1430. (c) Olah, G. A.; Liang, G. *Ibid.* **1976**, *98*, 3033. (d) Olah, G. A.; Staral, J. A. *Ibid.* **1976**, 6290. See also: Meier, G. *Angew. Chem.* **1988**, *100*, 317.

Structures of Ag_2X^+ and Cu_2X^+ Ions: Comparison of Theoretical Predictions with Experimental Results from Mass Spectrometry/Mass Spectrometry

R. A. Flurer and K. L. Busch*

Contribution from the School of Chemistry and Biochemistry, Georgia Institute of Technology, Atlanta, Georgia 30332. *Received April 26, 1989. Revised Manuscript Received January 3, 1991*

Abstract: Daughter ion MS/MS mass spectra have been recorded for Ag_2X^+ and Cu_2X^+ parent ions in which X is H, CH_3, O, or CO. Consideration of the dissociation processes observed suggests the prevalence of certain ion structures out of the several possible for these combinations of atoms. The suggested structures are compared with theoretical predictions based on Hartree-Fock SCF calculations using the relativistic ECP approximation. Present theoretical results agree with the rationalizations of the daughter ion MS/MS experiment in the assignment of a linear structure to Ag_2H^+, Ag_2O^+, and Cu_2O^+. Theoretical predictions of linear $Ag_2CH_3^+$ and $Cu_2CH_3^+$ are also supported by experimental work with mass spectrometry/mass spectrometry. Bent geometries are predicted for Ag_2CO^+ and Cu_2CO^+ by the calculations performed.

Introduction

Mass spectrometry/mass spectrometry (MS/MS) is a powerful tool for ion structure elucidation.[1] To record a daughter ion MS/MS spectrum, a parent ion of specified mass is selected from all ions formed in the source of the mass spectrometer, excited

* Address correspondence to this author.

(1) Busch, K. L.; Glish, G. L.; McLuckey, S. A. *Mass Spectrometry/Mass Spectrometry: Techniques and Application of Tandem Mass Spectrometry*, VCH Publishers: New York, 1988.

0002-7863/91/1513-3656$02.50/0

by collision with a neutral target gas, and the resultant fragment ions (daughter ions) analyzed in a second stage of mass analysis. The parent ions are the precursors to the daughter ion fragments. The terminology emphasizes the direct relationship of one ion to the other and can be extended in either direction. Extensive reviews of the applications of MS/MS in the determination of ion structure are available.[2,3] Many of the applications of MS/MS have been in the quantitative determination of specific compounds in complex mixtures or in structural studies of organic and biological molecules. In structural applications, structures determined by MS/MS can often be corroborated by other structural methods, particularly nuclear magnetic resonance spectrometry.

A smaller body of work deals with MS/MS spectra measured for coordination compounds and organometallic molecules. Still, the compound structures so established are supported with the use of other analytical methods. For very small molecules, there is some reasonable probability that the structure of the ion may differ from that of a neutral precursor or, in fact, that there may be no neutral analogue of the ion studied. In this arena, the quality of structural information accessible with MS/MS is less clear. In the absence of other methods of structural confirmation by experiment, the use of theoretical methods can be undertaken to provide the basis of comparison for MS/MS data. This is the purpose of the present paper, as applied to a series of Ag_2X^+ and Cu_2X^+ parent ions in which X is H, CH_3, O, or CO.

Busch et al.[4] have reported the daughter ion MS/MS spectra of parent ions generated from several silver carboxylate complexes, with particular emphasis on parent ions containing two silver atoms. On the basis of the observed fragmentation pathways, it was concluded that some of the parent and fragment ions contained metal–metal bonds. These conclusions were based on whether or not a given ion was present in the *parent* ion MS/MS spectrum of the Ag_2^+ dimer ion. In measurement of the parent ion MS/MS spectrum, the second-stage mass analyzer is set to pass a particular daughter ion mass through to the detector of the instrument. The first-stage mass analyzer is scanned across its range to generate a spectrum of all parent ions that dissociate to the specified daughter ion, viz., a parent ion MS/MS spectrum. The basic assumption for the conclusions is that ions that contain metal–metal bonds should dissociate to form Ag_2^+ and that those ions that lack a metal–metal bond should not dissociate to the silver dimer ion. It was therefore concluded that the structures of the species $Ag_2CH_3^+$, Ag_2O^+, and Ag_2CO^+ probably contain metal–metal bonds and that Ag_2H^+ does not contain a metal–metal bond.

The results of MS/MS cannot provide proof of ion structure, nor can it be assumed that an ion of specified mass should consist of only one structure. The interpretation of MS/MS spectra, as for mass spectra, is an exercise in rationalization. An implicit assumption of one structure for an ion of specified mass is often made based on an analysis of the energetics and kinetics of the mass spectrometer. Since the ion will possess a most stable and preferred form, the ion will generally rearrange until it reaches that configuration, assuming that it possesses sufficient time and energy to do so.

DeKock et al.[5] have recently calculated the equilibrium geometries, fragmentation energies, and ionization energies of Ag_2H^+ and $Ag_2CH_3^+$ using the Hartree–Fock–Slater (HFS)[6] method. DeKock et al. concluded that both of these ions are bent and may reasonably be expected to contain metal–metal bonds. Gaspar and Tamassy-Lentei[7] have also studied the Ag_2H^+ ion using a simple molecular pseudopotential method and have also concluded that the Ag_2H^+ ion is bent. However, the latter authors do not speculate on the existence of a metal–metal bond.

Because transition-metal atoms contain large numbers of electrons and the cost of computation increases rapidly with the number of electrons in the system (as n^4), computational methods for treating such atoms generally involve approximations that are not necessary for computations on molecules that contain only light atoms. The effective core potential (ECP) technique[8] involves the replacement of the inert core electrons with an effective one-electron potential that accurately reproduces the effect of the core electrons on the valence electrons. This significantly reduces the number of electrons requiring explicit treatment and reduces the problem to one involving only the valence electrons primarily responsible for bonding. ECP calculations also have the additional advantage of allowing one to easily incorporate the effects of relativity (RECPs), which are manifested as a decrease in bond lengths and an increase in binding energies.[9,10] These effects are due to the high velocities of the core electrons in heavy atoms, which are a large fraction of the speed of light. The net result is a contraction of the core electron density and, therefore, a contraction of the valence electron density because the valence orbitals must remain orthogonal to the core orbitals. The effect is most important for the core and valence s electrons. The effects on silver-containing molecules are small (0.05-Å change in bond length and 5–10 kcal/mol change in binding energy). The relativistic effects on copper-containing species are too small to be of importance, except in the most accurate calculations.

Recent work by Hay and Martin,[11] Hay and Rohlfing,[12] and Martin[13] has shown that the RECP technique is capable of producing results in close agreement with those from all-electron calculations that take into account relativistic effects using the perturbation theory or the Dirac–Hartree–Fock theory. Their studies have included a variety of silver-, palladium-, and platinum-containing species, and in each case their results were in close agreement with those obtained from corresponding all-electron calculations.

Theoretical studies have been carried out for the past decade on transition-metal atoms, dimers, trimers, and combinations with hydrogen, oxygen, and small organic groups such as the methyl group. Several different computational methods have been used, including the relativistic ECP method used in this paper. Exemplary citations to this work include a study of the structures and electron affinities of the dimers and trimers of the copper, silver, and gold by Bauschichler et al.[14] The positive ions of the first- and second-row transition-metal methyls (including copper and silver) have been similarly studied.[15] Accurate ab initio studies of the transition-metal hydrides and their positive ions have been completed by Schilling et al.,[16,17] Chong et al.,[18] Langhoff et al.,[19] and Petersson et al.[20] Comparative values for the results of the present calculations and those previously presented in the literature will be noted as they occur. To our knowledge, the

(2) Levsen, K.; Schwarz, H. *Mass Spectrom. Rev.* **1983**, *2*, 77.
(3) Cooks, R. G. In *Collision Spectroscopy*; Cooks, R. G., Ed.; Plenum Press: New York, 1979.
(4) Busch, K. L.; Cooks, R. G.; Walton, R. A.; Wood, K. V. *Inorg. Chem.* **1984**, *23*, 4093.
(5) DeKock, R. L.; van Zee, R. D.; Ziegler, T. *Inorg. Chem.* **1987**, *26*, 563.
(6) Connolly, J. W. D. In *Semiempirical Methods of Electronic Structure Calculation-Part A*; G. Segal, G. A.; Ed.; Plenum Press: New York, 1977.
(7) Gaspar, R.; Tamassy-Lentei, I. *Acta Phys. Acad. Sci. Hung.* **1981**, *50*, 343.
(8) Krauss, M.; Stevens, W. J. *Annu. Rev. Phys. Chem.* **1984**, *35*, 357.
(9) Christiansen, P. A.; Ermler, W. C.; Pitzer, K. S. *Annu. Rev. Phys. Chem.* **1985**, *36*, 407.
(10) Balasubramanian, K.; Pitzer, K. S. In *Ab initio Methods in Quantum Chemistry-I*; Lawley, K. P., Ed.; John Wiley and Sons: New York, 1987.
(11) Hay, P. J.; Martin, R. L. *J. Chem. Phys.* **1985**, *83*, 5174.
(12) Hay, P. J.; Rohlfing, C. M. In *Quantum Chemistry: The Challenge of Transition Metals and Coordination Chemistry*, Veillard, A., Ed.; D. Reidel Publishing Company: Boston, 1986.
(13) Martin, R. L. *J. Chem. Phys.* **1987**, *86*, 5027.
(14) Bauschichler, C. W., Jr.; Langhoff, S. A.; Partridge, H. *J. Chem. Phys.* **1989**, *91*, 2412.
(15) Bauschichler, C. W., Jr.; Langhoff, S. A.; Partridge, H.; Barnes, L. A. *J. Chem. Phys.* **1989**, *91*, 2399.
(16) Shilling, J. B.; Goddard, W. A., III; Beauchamp, J. L. *J. Phys. Chem.* **1987**, *91*, 5616.
(17) Shilling, J. B.; Goddard, W. A.; III; Beauchamp, J. L. *J. Am. Chem. Soc.* **1987**, *109*, 5565.
(18) Chong, D. P.; Langhoff, S. R.; Bauchichler, C. W., Jr.; Walch, S. P.; Partridge, H. *J. Chem. Phys.* **1986**, *85*, 2850.
(19) Langhoff, S. R.; Bauchichler, C. W.; Jr.; Petersson, L. G. M.; Partridge, H. *J. Chem. Phys.* **1987**, *86*, 268.
(20) Petersson, L. G. M.; Bauchichler, C. W.; Jr.; Langhoff, S. R.; Partridge, H. *J. Chem. Phys.* **1987**, *87*, 481.

results of DeKock et al. as described above represent the sole approach to the forms of Ag_2X^+ and Cu_2X^+, where X represents H or CH_3.

We have applied the RECP technique to the following silver-containing species found in the electron ionization mass spectrum of silver propionate: Ag_2H^+, Ag_2O^+, $Ag_2CH_3^+$, and Ag_2CO^+. We have also applied the ECP method to the corresponding copper-containing species using nonrelativistic ECPs. On the basis of the valence electron configurations for copper and silver ($d^{10}s^1$), which determine the bonding characteristics, one would expect that the corresponding species would mirror each other in terms of gross electronic structure and behavior in MS/MS experiments. The agreement, or lack thereof, between the calculated results for the copper- and silver-containing ions and the MS/MS experiments should be indicative of the reliability of each method and the extent to which they can be expected to corroborate one another.

This paper will discuss the results of these calculations and compare the results to those of DeKock et al. The calculated geometries will also be compared to predicted geometries based on interpretation of data obtained from MS/MS experiments. In addition, a discussion of the electronic structure and bonding for the M_2H^+, $M_2CH_3^+$, and M_2CO^+ (M = Ag or Cu) species will be presented. A fundamental reason for this study is that these small systems are prototypes for understanding the interaction of small molecules with transition-metal surfaces in such areas as heterogeneous catalysis.[21-23] This paper concentrates on the structures of ions that contain two metal atoms. An extensive body of work deals with the properties and reactions of single transition-metal atoms associated with varying number of carbonyls and with some systems involving two metal atoms.[24] However, we are unaware of studies of ions containing two silver or copper atoms in combination with carbonyl groups.

Method of Calculation

Full geometry optimizations were carried out at the Hartree–Fock SCF level of theory, using the ECP approximation and energy gradient techniques. The geometries and associated symmetry labels for each species studied are shown in Figure 1. The ab initio ECPs and associated valence basis sets of Hay and Wadt were used for silver and copper.[25] The silver ECP was relativistic (RECP) and included all electrons except the 4s and 4p outer core orbitals and the 5s, 5p, and 4d valence atomic orbitals, that is, a (28/19) RECP in the notation of Hay and Wadt. A corresponding (10/19) nonrelativistic ECP was used for copper, where 10 refers to the core electrons to be replaced by the ECP and 19 refers to the valence and outer core electrons left for explicit treatment by the SCF procedure. Effective core potentials that did not include the outer core atomic orbitals were used because the ordering of the energies of the molecular orbitals for some species was found to be sensitive to the type of ECP used, that is, a (28/19) RECP versus a (36/11) RECP in the case of silver, for example. The valence basis for the silver 5s and 5p atomic orbitals consisted of the primitive GTOs set forth by Hay and Wadt,[25] but the outermost two primitives were left uncontracted. The outer core atomic orbitals, 4s and 4p, were each represented by five contracted primitive Gaussian functions. The basis for the 4s and 4p valence atomic orbitals on copper also consisted of the three uncontracted primitives of Hay and Wadt.[25] For the 3d valence atomic orbitals on copper, the three innermost primitives of Hay and Wadt were contracted and the two most diffuse primitives were left uncontracted. As for silver, the outer core orbitals for copper, 3s and 3p, were represented by five contracted primitive Gaussians. Overall, the silver basis set consisted of a (5s5p/5s3p4d) basis contracted to [1s1p/3s3p3d], and the copper basis set consisted of a (5s5p/5s2p5d) basis contracted to [1s1p/3s2p3d]. The basis sets for C and O consisted of an STO4-31G* basis.[26] The transition-metal valence basis sets and the polarization functions for carbon and oxygen employed 6-fold Cartesian Gaussian d-type functions. The H basis set consisted of an STO6-31G** basis.[26] For all odd-electron species, the spin-unrestricted Hartree–Fock method was used. The HONDO codes of Dupuis et al. were used for all calculations.[26]

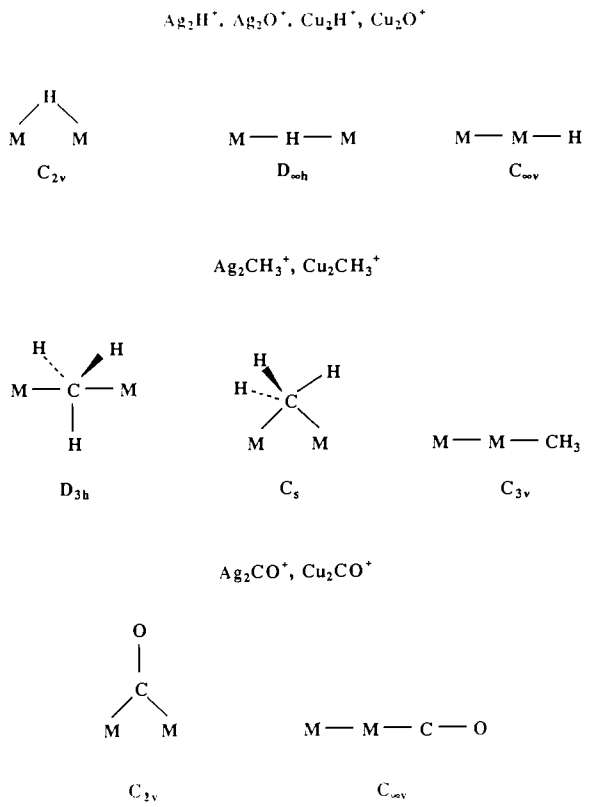

Figure 1. Geometries and associated point groups for the silver- and copper-containing ions of this study.

Experimental Section

Silver and copper propionate salts were synthesized by standard methods.[27] The propionate salts were chosen for specific study because the ions of interest (Ag_2X^+, as listed above) are most abundant in the mass spectra of the propionate salts. The results of Busch et al. were confirmed by repeating the original MS/MS experiments. As in the original work, a conventional 70-eV electron ionization source was used to produce ions for study. All MS/MS spectra were obtained on a Finnigan-MAT TSQ triple-quadrupole mass spectrometer. For all MS/MS spectra, the collision energy was held at 17 eV to distribute energy within a long-lived collision complex. Argon was used as the collision gas at a pressure observed to attenuate the parent ion beam by 50%. Samples were analyzed directly from a ballistically heated direct insertion probe. Mass spectra for copper propionate were recorded on a Kratos MS-80 RFAQ mass spectrometer under standard electron ionization conditions.

Results and Discussion

Geometric Structures of Ag_2H^+ and Cu_2H^+. Table I summarizes the optimized geometries obtained from the theoretical calculations for Ag_2H^+ and Cu_2H^+ ions, as well as values calculated for other diatomic species for comparison. Both Ag_2H^+ and Cu_2H^+ are predicted to have a linear ground-state structure $AgHAg^+$, and the Ag_2H^+ species is predicted to have a metal–H bond length 0.18 Å longer than that for the Cu_2H^+ species. The computations show that the linear topology Ag–Ag–H^+ is not stable and separates into Ag^+ and AgH fragments.

The linear ground-state geometries and the large distances between metal centers predicted by the present calculations preclude the existence of a metal–metal bond in either of these ions. Correspondingly, neither Ag_2H^+ nor Cu_2H^+ should be present in the parent ion MS/MS spectra of Ag_2^+ or Cu_2^+, respectively. The appropriate parent ion MS/MS spectra are given in Figures 2 (Ag_2^+) and 3 (Cu_2^+). In neither case is the $Metal_2H^+$

(21) McKee, M. L.; Worley, S. D. *J. Phys. Chem.* **1988**, *92*, 3699.
(22) McKee, M. L.; Dai, C. H.; Worley, S. D. *J. Phys. Chem.* **1988**, *92*, 1056.
(23) Nakatsuji, H.; Hada, M.; Yonezawa, T. *J. Am. Chem. Soc.* **1987**, *109*, 1902.
(24) Wronka, J.; Forbes, R. A.; Laukien, F. H.; Ridge, D. P. *J. Phys. Chem.* **1987**, *91*, 6450–6452.
(25) Hay, P. J.; Wadt, W. R. *J. Chem. Phys.* **1985**, *82*, 199.
(26) Poirier, R.; Kari, R.; Csizmadia, I. G. *Handbook of Gaussian Basis Sets*; Elsevier: New York, 1985.
(27) Bonner, W. A.; DeGraw, J. I. *J. Chem. Educ.* **1962**, *39*, 639.

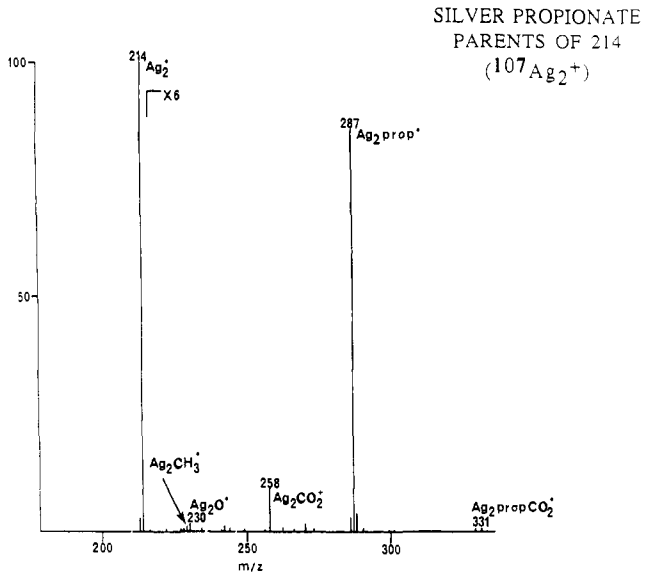

Figure 2. Parent ion MS/MS mass spectrum of the Ag_2^+ ion.

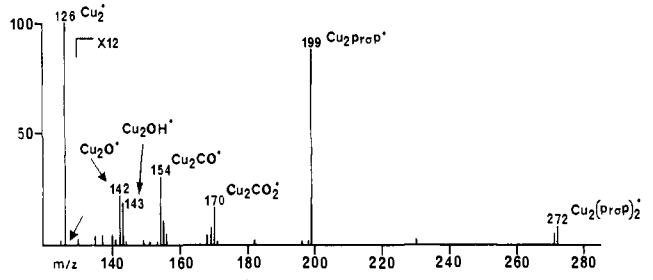

Figure 3. Parent ion MS/MS mass spectrum of the Cu_2^+ ion.

species observed in the parent ion MS/MS spectrum. The predicted linear ground-state geometry for each of these species is thus consistent with the MS/MS data.

Geometry optimizations for Ag_2H^+ and Cu_2H^+ ions indicate that each is linear because of strong steric repulsions between the transition-metal atoms. This repulsion results from the large partial positive charges on each metal atom (Tables II and III, supplementary material) and is not countered by the fact that the electronic component of the total energy is more favorable in the bent geometry. The situation can be described as a matter of the nuclear repulsion term overwhelming the electronic part of the total energy.

The calculated bond lengths for Ag_2H^+, Cu_2H^+, and other diatomic species are shown in Table I, with the experimental bond lengths in parentheses. Values derived for these species from other theoretical studies[14-20] are also included. The experimental bond lengths for the diatomic species suggest that this computational method predicts bond lengths that are 0.1–0.2 Å too long. The error is largest for species that contain metal–metal bonds, as shown by the predicted bond lengths of the silver and copper dimers. The experimental value for the silver dimer is not a directly measured experimental value but was obtained by interpolating between the known values for the copper and gold species. Martin[13] has shown that this error can be easily corrected by including the effects of electron correlation through the perturbation theory to second order, which avoids the size consistency problem of truncated configuration interaction treatments.

For the Ag_2H^+ species, DeKock et al.[5] predict a bent ground-state geometry $AgHAg^+$ with a central bond angle of 115° and an Ag–H bond length of 1.69 Å, which is 0.13 Å shorter than our calculated bond length. The bent ground-state structure for Ag_2H^+ and the overlap populations suggest the presence of a metal–metal bond, which is inconsistent with the absence of this species in the parent ion MS/MS spectrum of the silver dimer ion. Their computations also predict that the dissociation of Ag_2H^+ to Ag_2^+ is the least endothermic fragmentation pathway (58 kcal/mol or 2.5 eV) for this ion, and so such a process might reasonably be expected.

It is certainly difficult to compare *directly* the results of experiments and calculations or to compare the results of calculations based on different assumptions or incorporating differing levels of approximations. We acknowledge this difficulty, echoing early concerns of DeKock et al.[5] In any calculational method, the results reflect the details of the program structure and the input parameters. For instance, DeKock predicts a bent geometry for Ag_2H^+, but rovibronic excitation of the nascent ion may cause it to not retain the (bent) ground-state structure and to instead assume a linear excited state, which is calculated to be only 4 kcal/mol higher in energy. DeKock et al. state that there is no barrier for interconversion of the two geometries. There is enough energy available in the collisional activation used in the MS/MS experiment (62 kcal/mol for Ag_2H^+ incident on Ar collision gas at the stated collision energy for a center-of-mass calculation) for such an isomerization process to occur, since up to several percent of the translational energy can be converted into internal energy of the parent ion.[1] However, it does not seem likely that the entire population of ions would assume this higher energy geometry upon

Table I. Calculated Geometries for Silver- and Copper-Containing Species[e]

species	point group	parameter	value
Ag_2H^+	$D_{\infty h}$	r(Ag–H)	1.82
Ag_2O^+	$D_{\infty h}$	r(Ag–O)	2.19
	$C_{\infty v}$	r(Ag–Ag)	3.03
		r(Ag–O)	3.39
Ag_2CO^+	C_{2v}	r(Ag–Ag)	4.61
		r(Ag–C)	2.54
		r(C–O)	1.13
		∠AgCAg	129.9
$Ag_2CH_3^+$	D_{3h}	r(Ag–C)	2.37
		r(C–H)	1.08
	C_s	r(Ag–Ag)	2.97
		r(Ag–C)	2.39
		$r(C–H_a)$	1.086
		$r(C–H_b)$	1.09
		∠AgCAg	77.0
		$∠H_aCH_b$	103.8
		$∠H_bCH_b$	109.4
Ag_2	$D_{\infty h}$	r(Ag–Ag)	2.72 (2.48)[a,b]
AgH	$C_{\infty v}$	r(Ag–H)	1.71 (1.62)[c]
AgO	$C_{\infty v}$	r(Ag–O)	2.05 (2.00)[c]
Cu_2H^+	$D_{\infty h}$	r(Cu–H)	1.64
Cu_2O^+	$D_{\infty h}$	r(Cu–O)	1.94
	$C_{\infty v}$	r(Cu–Cu)	2.96
		r(Cu–O)	1.82
Cu_2CO^+	C_{2v}	r(Cu–Cu)	3.95
		r(Cu–C)	2.17
		r(C–O)	1.15
		∠CuCCu	131.0
$Cu_2CH_3^+$	D_{3h}	r(Cu–C)	2.12
		r(C–H)	1.09
	C_s	r(Cu–Cu)	2.68
		r(Cu–C)	2.12
		$r(C–H_a)$	1.09
		$r(C–H_b)$	1.10
		∠CuCCu	78.3
		$∠H_aCH_b$	102.0
		$∠H_bCH_b$	107.5
Cu_2	$D_{\infty h}$	r(Cu–Cu)	2.41 (2.22)[d]
CuH	$C_{\infty v}$	r(Cu–H)	1.56 (1.46)[c]

[a] Experimental values are given in parentheses. [b] Srdanov, V. I.; Pesic, D. S. *J. Mol. Spectrosc.* **1981**, *90*, 27. Maclean, A. D. *J. Chem. Phys.* **1983**, *79*, 3392. [c] Huber, H.; Herzberg, G. *Molecular Spectra and Molecular Structure. IV. Constants of Diatomic Molecules*; Van Nostrand Reinhold, New York, 1979. [d] Preuss, D. R.; Pale, S. A.; Gole, J. L. *J. Chem. Phys.* **1979**, *71*, 3553. Gole, J. L.; English, J. H.; Bondybey, V. E. *J. Phys. Chem.* **1982**, *86*, 2560. [e] Distances are given in angstroms and angles are given in degrees.

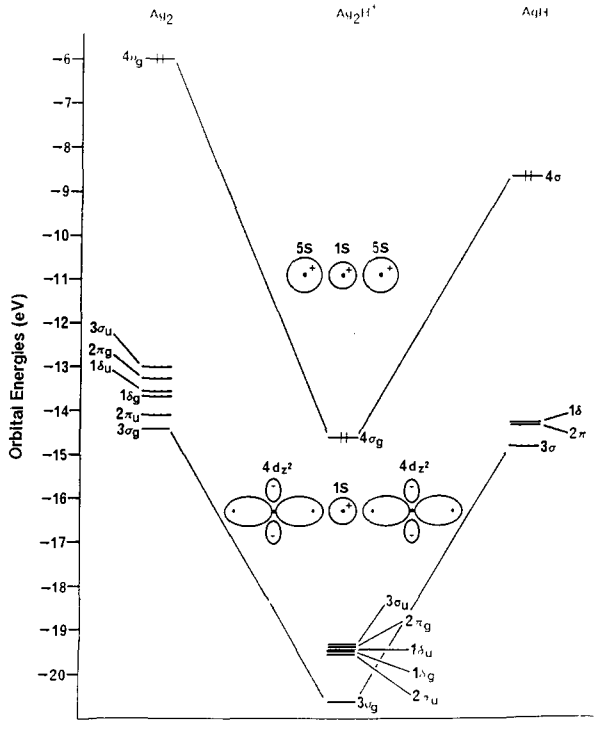

Figure 4. Molecular orbital correlation diagram for Ag_2, AgH, and Ag_2H^+.

collisional activation. Since the two geometries are so close in energy, and there is no barrier to interconversion, one would expect a mixture of the two geometries and that at least some of the ions leaving the reaction region would have the bent geometry necessary for the facile elimination of the central hydrogen atom. The fact that Ag_2H^+ is not observed at *all* to dissociate to Ag_2^+ suggests that this explanation is not valid. Additionally, the present calculations show that a bent (C_{2v}) stationary point does not exist on the Ag_2H^+ potential energy surface; a geometry optimization with a bent starting geometry will converge to the linear geometry given in Table I.

A possible explanation for the discrepancy between the results of the present computations for Ag_2H^+ and those of DeKock et al. is that the HFS method can predict binding energies that are too large in some cases.[28-30] If this were the case for the supposed metal–metal bond in Ag_2H^+, then the HFS method would predict that stabilization gained by formation of a metal–metal bond would offset the destabilizing effect of steric repulsion between the two positively charged metal centers. The HFS method would then predict a bent ground-state geometry. Conversely, electron correlation effects not included in our work could alter the energies and preferred structures of the ions explored in the present studies.

In support of the present results, we note that previous theoretical work[31-33] on the Li_2H^+ ion has shown that it has a linear ground-state geometry because of the steric repulsion between the positively charged metal atoms, in spite of the fact that the electronic part of the total energy is more favorable in a bent geometry. This is the same situation found in the present calculations for the Ag_2H^+ ion. The difference between the experimental bond energies for Li_2 (24 kcal/mol) and Ag_2 (38 kcal/mol) is only 14 kcal/mol; this difference may not be large enough to compensate for the steric repulsion in Ag_2H^+ and cause the formation of a metal–metal bond in the Ag_2H^+ ion. Finally, the present results are consistent with the experimental data for Ag_2H^+. Our calculated results for Cu_2H^+ are also consistent with the corresponding MS/MS data.

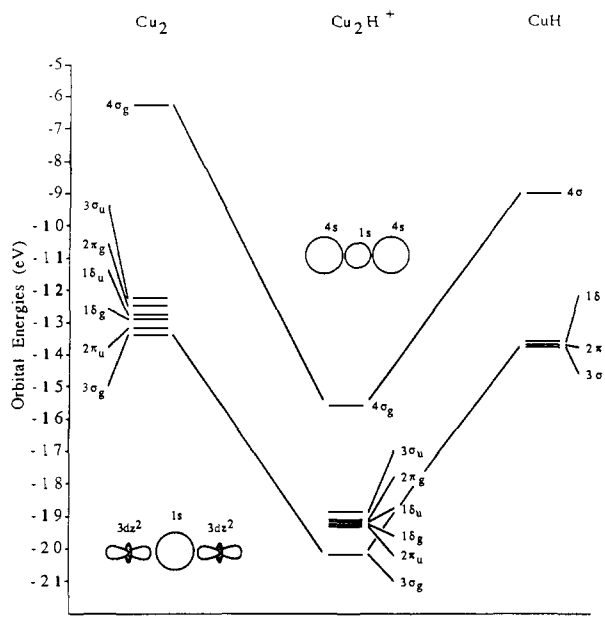

Figure 5. Molecular orbital correlation diagram for Cu_2, CuH, and Cu_2H^+.

Electronic Structures of Ag_2H^+ and Cu_2H^+. Figures 4 and 5 show the molecular orbital correlation diagrams for M_2, M_2H^+, and MH based on the present calculations. On the basis of a detailed analysis of each molecular orbital (parameters available as supplementary material), the bonding for the M_2H^+ ions can be assigned to a pair of molecular orbitals; these are the $3\sigma_g$ and $4\sigma_g$ molecular orbitals. These primary bonding molecular orbitals are consistent with those determined by DeKock et al., who assigned the bonding in Ag_2H^+ to these molecular orbitals. The $3\sigma_g$ molecular orbital consists of overlap of the hydrogen 1s atomic orbital with the $4d_{z^2}$ ($3d_{z^2}$) atomic orbital on each metal atom. The $4\sigma_g$ molecular orbital consist of overlap of the hydrogen 1s atomic orbital with the 5s (4s) atomic orbital on each metal atom. The $3\sigma_u$ molecular orbital is the antibonding counterpart to the $3\sigma_g$ bonding molecular orbital. The molecular orbitals of π and δ symmetry are, of course, strictly nonbonding by symmetry; there are no atomic orbitals with these symmetries available on the hydrogen atom. Also, as noted above, the large metal–metal distances in each M_2H^+ ion preclude any direct metal–metal interaction in the proximity of the hydrogen atom. The stabilization of the molecular orbitals of the cation apparent in Figures 4 and 5 is simply due to the charge on the cation.

Another piece of important information that can be gleaned from the molecular orbital correlation diagram is the extent to which the metal d orbitals are involved in bonding with the hydrogen atom in M_2H^+ and MH. As noted by DeKock et al., the degree of stabilization of the $3\sigma_g^+$ molecular orbital in M_2H^+ and the 3σ molecular orbital in MH relative to the nonbonding π and δ orbitals is indicative of the degree to which the metal d orbitals are involved in bonding with the hydrogen atom. The separation in energy of the $3\sigma_g^+$ and the $2\pi_u$ molecular orbitals of Ag_2H^+ is 1.096 eV, and the corresponding value for Cu_2H^+ is 0.981 eV. This indicates that the 4d atomic orbitals of silver are somewhat more involved in bonding with the hydrogen atom in Ag_2H^+ than are the 3d atomic orbitals of copper in Cu_2H^+. The 4d atomic orbitals of silver are more diffuse than the 3d atomic orbitals of copper due to the larger number of core electrons in silver, which more effectively shield the valence electrons from the atomic nucleus.

(28) Baerends, E. J.; Rozendall, A. In *Quantum Chemistry: The Challenge of Transition Metals and Coordination Chemistry*; Veillard, A., Ed.; D. Reidel Publishing Company: Boston, 1986.
(29) Rosch, N.; Jorg, H.; Dunlap, B. I. In *Quantum Chemistry: The Challenge of Transition Metals and Coordination Chemistry*; Veillard, A., Ed.; D. Reidel Publishing Company: Boston, 1986.
(30) Ziegler, T.; Tschinke, V.; Versluis, L. In *Quantum Chemistry: The Challenge of Transition Metals and Coordination Chemistry*; Veillard, A., Ed.; D. Reidel Publishing Company: Boston, 1986.
(31) Raffenetti, R. C.; Ruedenberg, K. *J. Chem. Phys.* **1973**, *59*, 5978.
(32) Cardelino, B. H.; Eberhardt, W. H.; Borkman, R. F. *J. Chem. Phys.* **1986**, *84*, 3230.
(33) Jemmis, E. D.; Chandrasekhar, J.; Schleyer, P. V. R. *J. Am. Chem. Soc.* **1979**, *101*, 527.

This trend is also evident in the population analysis (supplementary material) for each ion. The total gross population in the copper 3d atomic orbitals is somewhat higher than that in the silver 4d atomic orbitals. The population analyses also reveal that the 5p and 4p atomic orbitals of silver and copper, respectively, are not important in the bonding of the M_2H^+ ions. However, it is obvious that the valence d orbitals are strongly involved in bonding with the central hydrogen atom in both M_2H^+ ions.

Geometric Structures of $Ag_2CH_3^+$ and $Cu_2CH_3^+$. As shown in Table I, two optimized geometries were found for the $M_2CH_3^+$ ions, one with a linear M–C–M framework (D_{3h}) and one with a bent M–C–M framework (C_s). For the $Ag_2CH_3^+$ ion, the linear D_{3h} ground-state geometry was calculated to be 4.96 kcal/mol lower in energy than the C_s bent geometry, contrary to the results of DeKock et al. Their computations predict a bent C_s ground-state geometry that is 6 kcal/mol lower in energy than the linear D_{3h} geometry, and they estimate that the barrier for interconversion between the two geometries is about 50 kcal/mol. From present calculations, the linear D_{3h} ground-state geometry was found to be 3.90 kcal/mol lower in energy than the bent C_s geometry for the $Cu_2CH_3^+$ ion. The linear M–M–CH_3^+ (C_{3v}) topology was not bound for either ion and in each case separated into M^+ and MCH_3 fragments. The M–C bond lengths for each ion are virtually the same in the D_{3h} and C_s geometries. The calculated M–C–M bond angle in the C_s geometry of the $Ag_2CH_3^+$ ion (77°) is identical with that predicted by the work of DeKock et al. The corresponding bond angle in the $Cu_2CH_3^+$ ion is predicted to be nearly the same (78.3°). The present calculations predict for the C_s geometry of $Ag_2CH_3^+$ a metal–metal distance that is 0.22 Å longer than that of DeKock et al. However, Baerends and Rozendall[28] have shown that the HFS method predicts bond lengths that are generally too short. This notwithstanding, it seems possible that a weak metal–metal interaction could exist in the bent geometry of this ion. The same situation should hold for the bent geometry of the $Cu_2CH_3^+$ ion.

A close examination of the parent ion MS/MS spectra in Figures 2 and 3 reveals that both $M_2CH_3^+$ ions dissociate, to a small but detectable extent, to the M_2^+ ion. Busch et al.[4] note that the daughter ion MS/MS spectrum of the $Ag_2CH_3^+$ ion contains the Ag_2^+ ion at 30% relative abundance and the Ag^+ ion at 100% relative abundance. The linear ground D_{3h} state predicted by the present calculations precludes direct fragmentation of the $M_2CH_3^+$ ions to form M_2^+ ions, and the bent ground-state geometry of DeKock et al.[5] makes the elimination of a methyl radical to form M_2^+ a facile fragmentation. However, the lower abundance of the Ag_2^+ ion relative to the Ag^+ ion in the daughter ion MS/MS spectrum of $Ag_2CH_3^+$ suggests a more complex path to fragmentation. The computational results of DeKock et al. predict a bent C_s ground-state geometry and identical (within computational error limits) calculated fragmentation energies for formation of Ag^+ and $AgCH_3$ (63 kcal/mol) and for formation of Ag_2^+ and CH_3 (64 kcal/mol). These results suggest that the Ag^+ and Ag_2^+ ions should have roughly equal relative abundances in the daughter ion MS/MS spectrum of the $Ag_2CH_3^+$ ion, which is obviously not the case. Because both fragmentation processes are primarily simple bond cleavages (two bonds are cleaved in each case) and involve very little motion of the CH_3 subunit, they should have similarly high activation energies[34] and similar kinetics for each fragmentation pathway.

A total of 58 kcal/mol of energy (the center-of-mass energy) is available for conversion to internal energy of the $Ag_2CH_3^+$ ion upon collision with an argon target atom. This is enough energy for a small fraction of the parent ion population to overcome the 50 kcal/mol barrier for isomerization of the linear D_{3h} ground-state geometry predicted by the present calculations to the bent C_s excited-state geometry. Once over this barrier, an ion would have the correct geometry needed for facile fragmentation to the Ag_2^+ ion. The total energy requirement for this process (64 kcal/mol) would be met by the translational energy converted to internal energy upon collision, plus whatever internal energy the parent ion had acquired during the ionization process itself.

Only a small fraction of the parent ion population will acquire enough energy upon collisional activation to overcome the barrier to isomerization and assume the bent geometry necessary for fragmentation to the Ag_2^+ ion. Low-energy collisional activation produces a distribution of ion internal energies that is characterized by a maximum at lower internal energies and a tail that falls off rapidly to the theoretical maximum (the center-of-mass energy) for transfer of translational energy to internal energy.[35] At a given collision energy, only a small fraction of the parent ions will receive an amount of internal energy via collision that approaches the total center-of-mass energy. Since a majority of parent ions will not be able to adopt the bent C_s geometry, most will not have the Ag_2^+ fragmentation channel open to them, and they will instead fragment to form Ag^+. These results predict a much higher relative abundance for the Ag^+ ion relative to the Ag_2^+ ion in the $Ag_2CH_3^+$ ion daughter ion MS/MS spectrum and a low abundance of the $Ag_2CH_3^+$ ion in the parent ion MS/MS spectrum of the Ag_2^+ ion, as observed in the MS/MS experiments. These arguments apply equally well to the $Cu_2CH_3^+$ ion.

Additional support for the correctness of linear D_{3h} ground-state geometry predicted for the $M_2CH_3^+$ ions by the present calculations can be found in the theoretical work of Jemmis et al.[33] for the $Li_2CH_3^+$ ion. Their computations showed that the linear D_{3h} geometry is favored by 2.5 kcal/mol over the bent C_s geometry primarily because of the steric repulsion between the metal atoms caused by the large positive charge (+0.712) on each metal atom. The similarity of the charges computed for the metal atoms in the $M_2CH_3^+$ ions by the present calculations (see the supplementary material) to those computed for the $Li_2CH_3^+$ ion suggests that the $M_2CH_3^+$ ions studied here should also have linear D_{3h} ground states for the same reason. As was the case for the M_2H^+ ions, a possible explanation for the bent C_s ground state predicted by DeKock et al. is that the HFS method overestimates the importance of the supposed metal–metal bond in the structure of the $Ag_2CH_3^+$ ion.

The arguments advanced to bring the theoretical predictions in line with the experimental results are not without restrictions. For instance, the initial distribution of D_{3h} and C_s states of the $M_2CH_3^+$ ions in the source is neither known nor specified, and this, among other factors, leads to uncertainty in the interpretation of the results.

Electronic Structures of $Ag_2CH_3^+$ and $Cu_2CH_3^+$. The major-component atomic orbitals that characterize each of the molecular orbitals of the $M_2CH_3^+$ ions have been determined (supplementary material). A detailed examination of each molecular orbital shows that the bonding in the two ions can be assigned to five of them; these are the $3a'_1$, $2e'$, $3a''_2$, and $4a''_2$ molecular orbitals. The $3a'_1$ molecular orbital is the a_1 fragment of the planar CH_3 unit and consists of the ($C_{2s} + H^1_{1s} + H^2_{1s} + H^3_{1s}$) linear combination. The $2e'$ degenerate pair consists of overlap of the carbon $2p_x$ atomic orbital with the metal d_{xz} atomic orbitals and overlap of the carbon $2p_y$ atomic orbital with the metal d_{yz} atomic orbitals. The hydrogen 1s atomic orbitals are also involved in each member of this degenerate pair. The $4e'$ degenerate pair are the corresponding antibonding molecular orbitals. The $3a''_2$ molecular orbital consists of interaction of the carbon $2p_z$ atomic orbital with the d_{z^2} atomic orbital on each metal atom, and the $4a'_1$ molecular orbital is the corresponding antibonding molecular orbital. The $2e''$ (d_{xz}, d_{yz}), $3e'$ (d_{xy}, $d_{x^2-y^2}$), and $3e''$ (d_{xy}, $d_{x^2-y^2}$) molecular orbitals consist of metal-centered nonbonding symmetry adapted linear combinations of atomic orbitals.

The $4a''_2$ molecular orbital involves mainly overlap of the carbon $2p_z$ atomic orbital with the valence s atomic orbital on each metal atom. However, it appears that the metal valence p_z atomic orbital (5p for Ag and 4p for Cu) is also involved, but to a much smaller extent. The population analysis for each ion indicates that the p_z orbitals contain a significant amount of electron density, ap-

(34) Levsen, K. *Fundamental Aspects of Organic Mass Spectrometry*; Verlag Chemie: New York, 1978.

(35) Wysocki, V. H.; Kenttamaa, H. I.; Cooks, R. G. *Int. J. Mass Spectrom. Ion Proc.* **1987**, *75*, 181.

proximately 0.1 in each case. This indicates that perhaps the valence s and p_z atomic orbitals on each metal center are hybridizing.

The population analysis also reveals the overall significance of the metal d orbitals in the bonding for each ion; the total population of the silver d atomic orbitals in 9.853 and the corresponding value for copper is 9.969. The value for the free atom in each case is 10.000. These values indicate that the d atomic orbitals of silver are more important in the context of bonding to the CH_3 unit than are the copper d atomic orbitals. As was the case for the M_2H^+ ions, this is in accord with the more diffuse nature of the silver d atomic orbitals. DeKock et al. also note the importance of the silver d atomic orbitals in the bonding of the $Ag_2CH_3^+$ ion.

Geometric Structures of Ag_2CO^+ and Cu_2CO^+. On the basis of the electronic structure of the CO molecule (vide supra), the only plausible geometries for the M_2CO^+ ions are the bent C_{2v} and linear M–M–CO^+ geometries shown in Figure 1. The bent C_{2v} geometry is predicted to be the ground-state geometry for each ion, and the linear topology is not bound; that is, the linear structure separates into M^+ and MCO fragments as the geometry optimization proceeds. The M–C–M bond angles are nearly the same for each ion; this angle is predicted to be 129.9° for the Ag_2CO^+ ion and 131.0° for the Cu_2CO^+ ion. The C–O bond length is also nearly the same for each ion.

The large metal–metal distances (compared to the metal dimers) for each ion prevent the existence of a metal–metal bond in the ground-state geometry of either ion. However, the absence of a metal–metal bond would not necessarily prevent the formation of a metal–metal bond in a three-membered transition state for the elimination of a neutral molecule of CO. The bent ground-state geometry would allow the easy formation of such a bond through the symmetric bending mode of the M–C–M bond angle, given that a sufficient number of vibrational quanta were localized in this mode after collisional activation to bring the metal atoms close together. This explains the low relative abundance of the M_2CO^+ ion observed in the baseline of the M_2^+ ion parent ion MS/MS spectra (Figures 2 and 3). However, close examination of the MS/MS spectra reveals that the Cu_2CO^+ ion is more abundant in the Cu_2^+ ion parent ion MS/MS spectrum. (The comparison is between the abundance observed in the Cu_2^+ ion parent ion MS/MS spectrum versus twice that shown in the Ag_2^+ ion parent ion MS/MS spectrum.) This greater abundance is simply due to the greater center-of-mass energy available in the collision of a Cu_2CO^+ ion with an argon target atom compared to the Ag_2CO^+ ion incident on an argon target atom.

Electronic Structures of Ag_2CO^+ and Cu_2CO^+. The bent C_{2v} ground-state structure predicted for the M_2CO^+ ions is a consequence of the unique electronic structure of the carbon monoxide (CO) molecule. The CO molecule is a good π acceptor as well as a good σ donor. The 2σ molecular orbital consists of a lone pair of electrons localized on the carbon atom and is responsible for the σ-donor property of the CO molecule. The $1\pi^*$ degenerate pair of antibonding molecular orbitals is also strongly weighted on the carbon atom and is responsible for the π-acceptor character of the CO molecule.[36,37] The CO molecular orbitals are responsible for bonding with the metal atoms in the M_2CO^+ ions.

A detailed analysis of the molecular orbitals of the M_2CO^+ ions (supplementary material) shows that in each case the bonding can be localized to the $6a_1$ and $8b_2$ molecular orbitals. The $6a_1$ molecular orbital consists of overlap of the carbon lone pair with a hybrid atomic orbital on each metal atom (d_{y^2} mixed with d_{yz}). It is believed that the d_{yz} atomic orbital mixes with the d_{y^2} atomic orbital on each metal center to produce a hybrid orbital directed toward the carbon atom lone pair, which would presumably allow better orbital overlap. The $8b_2$ molecular orbital, which contains a single unpaired electron, incorporates overlap of the metal valence s atomic orbitals with the π^*_y component of the antibonding degenerate pair of the CO molecule. Because this molecular orbital contains only one electron, it could be described as a three-center, one-electron bond.

Other molecular orbitals of interest are the $4a_1$, $5a_1$, $2b_1$, $4b_2$, and $9a_1$ molecular orbitals. The $4a_1$ molecular orbital is the CO molecule σ bond. The $5a_1$ molecular orbital is primarily the oxygen atom lone pair of the CO molecule. The $2b_1$ and $4b_2$ molecular orbitals consist of the two π bonds of the CO molecule. The $9a_1$ molecular orbital is antibonding in nature and corresponds to the $6a_1$ bonding molecular orbital discussed above.

The population analyses for the M_2CO^+ ions also reveal some interesting information about the bonding in these two ions. The d atomic orbital populations show the same trend observed for the other ions discussed thus far. The d atomic orbitals of silver are much more involved in bonding to the CO molecule in the Ag_2CO^+ ion than the d atomic orbitals of copper are in the Cu_2CO^+ ion, which is a consequence of the more diffuse nature of the silver 4d atomic orbitals. This indicates that the copper atoms in the Cu_2CO^+ ion are bound to the CO molecule primarily by the three-center, one-electron bond found in the $8b_2$ molecular orbital. This is not the case for the Ag_2CO^+ ion because of the more extensive involvement of the silver 4d atomic orbitals.

Geometric Structures of Ag_2O^+ and Cu_2O^+. Two optimized geometries were found for each of the M_2O^+ ions (Table I); the linear M–O–M^+ geometry is the ground-state geometry in each case. For the Ag_2O^+ ion, the linear Ag–Ag–O^+ geometry was found to be 28 kcal/mol higher in energy than the ground-state geometry. For the Cu_2O^+ ion, the linear Cu–Cu–O^+ geometry was found to be 70 kcal/mol higher in energy than the ground-state geometry. For both ions, the M–M–O^+ topology incorporates a relatively long metal–metal bond, as compared to the metal dimers. The long metal–metal bonds indicate that the interaction between the metal atoms is weak. Higher level calculations would be necessary to judge the complete character of this weak interaction.

The M–M–O^+ topology is interesting because it is the only M–M–X^+ topology studied that is bound. The prediction of a bound structure also explains the presence of the M_2O^+ ion in each of the parent ion MS/MS mass spectra for the metal dimer ions. As was the case for the M_2H^+ ions, the linear M–O–M^+ ground state lacks a metal–metal bond, and dissociation of M_2O^+ ions to M_2^+ ions is not expected. Although the present calculations cannot predict the barrier height for isomerization of the linear M–O–M ground-state geometry to the linear M–M–O excited-state geometry, there is probably enough center-of-mass energy available upon collisional activation (58 kcal/mol for the Ag_2O^+ ion and 86 kcal/mol for the Cu_2O^+ ion) for each ionic species to allow a fraction of the ground-state population to isomerize to the higher energy linear geometry. Once in the linear M–M–O^+ geometry, the fragmentation of the ion to the metal dimer ion would be quite facile, requiring only the cleavage of the M–O bond. As was the case for the M_2CO^+ ions, the greater relative abundance of the Cu_2O^+ ion compared to the Ag_2O^+ ion in the parent ion MS/MS spectra is due to the greater center-of-mass energy available for the collisional activation of the Cu_2O^+ ion.

Conclusions

The Hartree–Fock SCF method, using effective core potentials to replace the core electrons of transition metals, provides geometric predictions for transition-metal-containing ionic species that are consistent with the results of MS/MS experiments. The M_2H^+ ions are predicted to have linear ground-state structures, which is consistent with the absence of these two ions in the corresponding M_2^+ ion parent ion MS/MS spectra. The $M_2CH_3^+$ ions are also predicted to have a linear M–C–M ground-state geometry, which at first seems inconsistent with the presence of this ion in each M_2^+ parent ion MS/MS spectrum but is explained by the excitation of a small fraction of the linear ground-state ions, upon collisional activation, to the bent excited-state geometry. Once in this excited state, the ions would have the correct geometry to dissociate to the M_2^+ ion.

The M_2CO^+ ions are predicted to have bent C_{2v} ground-state geometries. The large metal–metal distance in each of these

(36) Cotton, F. A.; Wilkinson, G. *Advanced Inorganic Chemistry: A Comprehensive Text*, 4th ed.; John Wiley and Sons: New York, 1989.
(37) Albright, T. A.; Burdett, J. K.; Whangbo, M. *Orbital Interactions in Chemistry*, Wiley: New York, 1985.

species prevents the existence of metal-metal bonds in the ground-state geometry. However, the symmetric bending motion of the M-C-M framework should allow the two metal atoms to form a three-membered transition state for the elimination of a CO molecule. Localization of a sufficient number of vibrational quanta in this bending mode is more likely for the copper species. The greater center-of-mass energy available for collisional activation of the copper species explains the greater abundance of the Cu_2CO^+ ion in the Cu_2^+ ion parent ion MS/MS spectrum compared to the Ag_2CO^+ ion in the Ag_2^+ ion parent ion MS/MS spectrum.

The M_2O^+ ions are predicted to have linear M-O-M ground-state structures, which precludes the existence of a metal-metal bond. The presence of this ion in the metal dimer ion parent ion MS/MS spectra is explained by rearrangement of a small fraction of the ground-state ion population to an excited-state M-M-O geometry. This excited-state geometry requires only simple cleavage of the M-O bond to form the metal dimer ion.

The present computational method also provides useful information about electronic structures of transition-metal-containing ionic species. With the exception of the Cu_2CO^+ ion, the copper species examined in this study are bound primarily by three-center, two-electron bonds. Since they contain an odd number of electrons, the metal atoms in the Cu_2CO^+ ion are bound to the CO molecule by the equivalent of a three-center, one-electron bond. The 3d atomic orbitals are not as involved because they are much less diffuse than the 4s atomic orbitals and are buried inside the 4s atomic orbitals. In contrast, the bonding in the silver-containing species studied cannot be described in this way. The same three-center, two-electron and three-center, one-electron bonds exist in the silver-containing species. However, the 4d atomic orbitals are more involved in the bonding. The 4d atomic orbitals of silver are much more diffuse than the 3d atomic orbitals of copper because of the larger number of core electrons in a silver atom. The core electrons more effectively shield the 4d electrons from the nucleus, thus making them more diffuse.

The predictive results of this work suggest that the interpretation of MS/MS data is not always straightforward. The simple presence or absence of an ion formed in a specific fragmentation pathway may lead to erroneous structural assumptions in situations in which excited-state geometries can be accessed. For instance, Busch et al.[4] deduced that the $Ag_2CH_3^+$ ion incorporates a metal-metal bond; the present computational results suggest that this is *not* the case. Sufficient energy is available in the collisional activation to form alternate higher energy ion structures.

Overall, this work shows that the ECP method can predict ionic geometries and excited-state geometries that are consistent with MS/MS data and that aid in its interpretation. With more sophisticated methods of incorporating relativistic effects on bonding into the calculational methods for compounds containing heavy elements, as described by Ziegler et al.,[38] increased use of these methods for structure investigations can be foreseen.

Acknowledgment. We thank R. G. Cooks at Purdue University for the use of the triple-quadrupole mass spectrometer. This work is part of the Ph.D. Thesis of R.A.F. at Indiana University.

Registry No. Ag_2H^+, 81900-29-0; Ag_2O^+, 133071-33-7; Ag_2CO^+, 133071-34-8; $Ag_2CH_3^+$, 106471-89-0; Ag_2, 12187-06-3; AgH, 13967-01-6; AgO, 1301-96-8; Cu_2H^+, 81900-28-9; Cu_2O^+, 116873-91-7; Cu_2CO^+, 133071-35-9; $Cu_2CH_3^+$, 133071-36-0; Cu_2, 12190-70-4; CuH, 13517-00-5.

Supplementary Material Available: Tables 2-13 giving population analyses and major components of molecular orbitals for Ag_2H^+, Cu_2H^+, $Ag_2CH_3^+$, $Cu_2CH_3^+$, Ag_2CO^+, and Cu_2CO^+ (20 pages). Ordering information is given on any current masthead page.

(38) Ziegler, T.; Snijders, J. G.; Baerends, E. J. *J. Chem. Phys.* **1981**, *74*, 1271.

ESCA Studies of Phase-Transfer Catalysts in Solution: Ion Pairing and Surface Activity

R. Moberg,[†] F. Bökman,[‡] O. Bohman,[‡] and H. O. G. Siegbahn*,[†]

Contribution from the Department of Physics, Box 530, and the Department of Organic Chemistry, Box 531, University of Uppsala, S-751 21 Uppsala, Sweden. *Received June 18, 1990. Revised Manuscript Received December 21, 1990*

Abstract: Phase-transfer catalysts in solution have been studied by means of electron spectroscopy. Different anion-cation distributions at the surface were found depending on the anion identity. Thus, tetrabutylammonium perchlorate and tributyl-3-iodopropylammonium iodide show strong evidence of the formation of contact ion pairs at the surface. Conversely, the tetrabutylammonium nitrate and chloride show a more diffuse character of the anion distribution with respect to the surface. The observed differences in surface structure between the salts correlate with the variation in transfer coefficients from aqueous to organic phase.

Introduction

Phase-transfer catalysis with tetraalkylammonium salts is an extremely powerful method in organic synthesis and has been employed in a multitude of applications since the pioneering work of Makosza,[1,2] Starks,[3] and Brändström.[4] The tetrabutylammonium ion is one of the most efficient catalytic agents in this group and has been the subject of several investigations using various methods, such as conductometric,[5-10] Raman,[11] IR,[12] and NMR[13] techniques. Measurements of electrolyte molar volume,[14]

[†] Department of Physics.
[‡] Department of Organic Chemistry.

(1) Makosza, M.; Serafinowa, B. *Rocz. Chem.* **1965**, *39*, 1223.
(2) Makosza, M.; Wawrzyniewicz, W. *Tetrahedron Lett.* **1969**, 4659.
(3) Starks, C. M. *J. Am. Chem. Soc.* **1971**, *93*, 195.
(4) Brändström A. *Preparative Ion Pair Extraction, an Introduction to Theory and Practice*; Apotekarsocieteten, Hässle Läkemedel: Stockholm, 1974.
(5) Sigvartsen, T.; Gestblom, B.; Noreland, E.; Songstad, J. *Acta Chem. Scand.* **1989**, *43*, 103.

0002-7863/91/1513-3663$02.50/0